Mol Cell Biochem (2014) 392:39–48
DOI 10.1007/s11010-014-2016-4

The effect of combined regulation of the expression of peroxisome proliferator-activated receptor-γ and calcitonin gene-related peptide on alcohol-induced adipogenic differentiation of bone marrow mesenchymal stem cells

Jinfeng Li · Yisheng Wang · Yuebai Li · Junkui Sun · Guoqiang Zhao

Received: 10 December 2013 / Accepted: 28 February 2014 / Published online: 15 March 2014

Abstract Studies have shown that alcohol can upregulate the expression of peroxisome proliferator-activated receptor-γ (PPARγ) gene in bone marrow mesenchymal stem cells (BMSCs). High expression of PPARγ can promote adipogenic differentiation of BMSCs, and reduce their osteogenic differentiation. Abnormal proliferation of adipocytes and fatty accumulation in osteocytes can result in high intraosseous pressure and disturbance of blood circulation in the femoral head, which induces osteonecrosis of the femoral head (ONFH). Downregulation of PPARγ is efficient in inhibiting adipogenesis and maintaining osteogenesis of BMSCs, which might potentially reduce the incidence of ONFH. Calcitonin gene-related peptide (CGRP) is a neuropeptide gene which has been closely associated with bone regeneration. In this study, we aimed to observe the effect of combined regulation of the expression of PPARγ and CGRP genes on alcohol-induced adipogenic differentiation of BMSCs. Our results demonstrated that simultaneous downregulation of PPARγ and upregulation of CGRP was efficient in suppressing adipogenic differentiation of BMSCs and promoting their osteogenic differentiation. These findings might enlighten a novel approach for the prevention of ONFH.

J. Li · Y. Wang (✉) · J. Sun
Department of Orthopaedic Surgery, The First Affiliated Hospital of Zhengzhou University, Zhengzhou 450052, Henan, China
e-mail: wangyisheng@zzu.edu.cn

Y. Li · G. Zhao
Basic Medical College, Zhengzhou University, Zhengzhou 450001, Henan, China

Keywords RNA interference · Peroxisome proliferator-activated receptor-γ · Calcitonin gene-related peptide · Bone marrow mesenchymal stem cells · Differentiation

Introduction

Osteonecrosis of the femoral head (ONFH) is a common orthopedic clinical disease and is generally classified into traumatic and non-traumatic ONFH. Non-traumatic ONFH, often seen in young patients, can be aggravated by approximately 40 etiologic factors. Alcohol abuse is one of the most common seen among them [1]. Bone marrow mesenchymal stem cells (BMSCs) have the potential to differentiate into many lineages [2, 3], such as osteoblasts, adipocytes, fibroblasts, chondrocytes, and neurocytes [4–7]. Consequently, BMSCs could be widely applied in bone tissue engineering and in gene therapy for many diseases.

As a member of the ligand-activated nuclear transcription factor superfamily, peroxisome proliferator-activated receptor-γ (PPARγ) is known to be an adipogenic transcription factor. PPARγ can induce pre-adipocytes to differentiate into adipocytes and is closely involved in the induction of adipogenesis [8–11]. Studies have shown that the development of ONFH is closely related to high expression of PPARγ [12, 13]. High expression of the PPARγ gene can also promote adipogenic differentiation of BMSCs and reduce their osteogenic differentiation. The alterations of BMSCs will increase fatty accumulation and lead to high intraosseous pressure in the femoral head. Eventually, blood circulation was blocked and ONFH started.

Calcitonin gene-related peptide (CGRP) is a neuropeptide gene which is related to bone growth and metabolism. CGRP-positive nerve fibers are abundantly distributed in

bone tissue, and play an important role in the regulation of bone formation and resorption [14, 15]. The CGRP receptor is found on the surface membrane of BMSCs. Studies have shown that CGRP-modified BMSCs can not only secrete high levels of biologically active exogenous CGRP, but also display an increased proliferation rate and osteogenic potential [16, 17].

In this study, the expressions of both the PPARγ and the CGRP genes were regulated in the presence of alcohol. Concomitant downregulation of the expression of PPARγ by a small interfering RNA and increased expression of CGRP inhibited the adipogenic differentiation of BMSCs and promoted their osteogenic differentiation. These findings might provide a novel experimental condition for the prevention or treatment of ONFH.

Materials and methods

Materials

The pGFP-V-RS vector was obtained from OriGene Technologies (Rockville, MD). This vector contains the U6 promoter and siRNA expressing unit of the multiple cloning site (MCS), as well as the CMV promoter and TGFP fusion protein-expressing unit of the MCS. Mouse anti-rabbit PPARγ polyclonal antibody; mouse anti-rabbit CGRP monoclonal antibody; mouse anti-rabbit Runx2 polyclonal antibody; mouse anti-rabbit osteocalcin (OC) polyclonal antibody; mouse anti-rabbit β-actin polyclonal antibody; goat anti-mouse IgG/enzyme; and monoclonal antibodies against CD29, CD34, CD44, CD45, and CD105 were all purchased from Abcam (Cambridge, UK). Enzyme-linked immunosorbent assay (ELISA) test kits for alkaline phosphatase, OC, laminin, and collagen type I were from R&D Systems (Minneapolis, MN). Fetal bovine serum (FBS) and low-glucose Dulbecco's modified Eagle medium (DMEM) were from Gibco/Life Technologies (Carlsbad, CA). Restriction endonucleases *Bam*H I, *Hin*d III, and *Mlu* I; alkaline phosphatase; and T4 DNA ligase were purchased from TaKaRa Bio Inc. (Shiga, Japan). The total RNA extraction kit was purchased from Omega Bio-Tek Inc. (Norcross, GA). RevertAid first strand cDNA synthesis kit was purchased from Thermo Scientific (Waltham, MA).

Construction of the recombinant vector

Two oligonucleotide chains of PPARγ siRNA were synthesized according to the principles of siRNA design, and the resulting PPARγ siRNA oligonucleotide sequences were positive sense strand 5′GATCGGCCTTTCACCAC CGTGGACTTCTCCAGCATCAAGAGTGCTGGAGAA GT CCACGGTGGTGAAAGGCGA3′ and anti-sense strand 5′AGCTTCGCCTTTCACCACCG TGGACTTCTCCAG CACTCTTGATGCTGGAGAAGTCCACGGTGGTGA-AAGGCC3′. After annealing, the double-stranded hairpin cDNA was ligated into the pGFP-V-RS vector to obtain the silencing vector pGFP-V-RS-siPPARγ, which can downregulate expression of the PPARγ gene. The open reading frame (ORF) cDNA of CGRP was also ligated into the pGFP-V-RS vector to obtain the expression vector pGFP-V-RS-exCGRP, which expresses the CGRP gene. Meanwhile the ORF cDNA of CGRP was cloned into the MCS downstream of the CMV promoter to obtain the double-gene vector pGFP-V-RS-siPPARγ-exCGRP, which can downregulate expression of the PPARγ gene and express the CGRP gene.

Culture and identification of BMSCs

Autologous primary BMSCs were harvested from the bone marrow of New Zealand white rabbits using lymphocyte separation medium by density gradient centrifugation. They were then suspended in low-glucose complete DMEM (containing 10 % FBS, 100 kU/mL penicillin, 100 mg/L streptomycin, 50 mg/L ascorbic acid, 1 mmol/L L-glutamine, and 20 mmol/L Hepes) and cultured at 37 °C in 5 % CO_2 in air. Medium was replaced with fresh culture medium after 3 days and subsequent medium changes were carried out every 2 days. The morphology and growth of BMSCs was observed daily by phase contrast using an inverted microscope. Subculture was performed when cells reached 70–80 % confluence.

Third passage cells in good condition were collected and a single-cell suspension was prepared. After washing 3 times with phosphate-buffered saline (containing 1 % BSA), a monoclonal antibody to CD29, CD34, CD44, CD45, or CD105 was added into each tube; a negative control was prepared in parallel. After incubating for 30 min at 4 °C, the cells were washed twice and the secondary antibody was added. The cells were then incubated for 30 min at 4 °C, then washed twice and analyzed by flow cytometry.

Transfection and grouping of BMSCs

Third passage BMSCs were collected into 15 mL centrifuge tubes, pooled, and counted. According to the electroporation requirement of BTX ECM 2001 for BMSCs, the final cell density was 2.0×10^7 cells/mL and 250 μL of cell suspension was added into the BTX electroporation cuvettes. The vector (10 μL of the double-gene vector pGFP-V-RS-siPPARγ-exCGRP, the silencing vector pGFP-V-RS-siPPARγ, the expression vector pGFP-V-RS-exCGRP, or empty pGFP-V-RS vector) was also added to the cuvettes. After transfection under a direct current and low-voltage pulse, BMSCs were seeded into 6-well plates and low-

glucose complete DMEM was added. The experiment was divided into 6 groups. Double Group: BMSCs were transfected with the double-gene vector pGFP-V-RS-siPPARγ-exCGRP, which can downregulate expression of PPARγ and express CGRP, and induced with alcohol. PPARγ Group: BMSCs were transfected with the silencing vector pGFP-V-RS-siPPARγ, which downregulates expression of PPARγ, and induced with alcohol. CGRP Group: BMSCs were transfected with the expression vector pGFP-V-RS-ex-CGRP, which expresses CGRP, and induced with alcohol. Control Group: BMSCs were transfected with the pGFP-V-RS vector, which was a blank vector and ineffective in regulating the expression of PPARγ and CGRP gene, and induced with alcohol. Model Group: BMSCs were induced with alcohol only. Normal Group: BMSCs were not transfected with any vector nor induced with alcohol. Alcohol at 0.09 mol/L was added to the culture medium of all groups requiring alcohol induction, and fresh alcohol was added every time the medium was replenished to a final concentration of 0.09 mol/L. The morphology and growth of BMSCs was observed by inverted phase-contrast microscopy daily until used for the experiments described below.

MTT proliferation assay

BMSCs in each group were seeded into 96-well plates (1×10^4 cells/well) and incubated with 20 μL of 5 mg/mL 3-(4, 5-dimethylthiazol-2-yl)-2, 5-diphenyltetrazolium bromide (MTT) for 4 h at 37 °C. After removing the supernatant, 150 μL of dimethylsulfoxide (DMSO) was added to each well and the absorbance was measured at a wavelength of 490 nm using a microplate reader.

Determination of the expression of PPARγ, CGRP, Runx2, and osteocalcin mRNA by RT-PCR

Total RNA was extracted from BMSCs using a Total RNA extraction kit (Omega) at day 7, and used as a template for cDNA synthesis using a RevertAid first strand cDNA synthesis kit. Expression of PPARγ, CGRP, Runx2, and OC mRNA was determined by TaqMan Real-Time PCR (TaqMan probe fluorescence detection), and the PCR primer sequences and probe used in this study were as follows: PPARγ: forward (f), 5′ TGACACAGAGATGCCGTTTTG 3′, reverse (r), 5′ CATCCATGACCGAGAGATCCA 3′, fluorescence probe sequence (probe), FAM 5′ CCCACCAACTTCGGGATCGGC 3′TAMRA; CGRP: f, 5′ TCATGGGCTTCCTCAAGTTCTC 3′, r, 5′ CACTGCGTGGAGGCTGTCT 3′, probe, FAM 5′ CTCTTAGCATCTTGGTCCTGTA 3′TAMRA; Runx2: f, 5′ TTCAGAACTGGGCCCTTT 3′, r, 5′ CTCAGTGAGGGATGAAATGC 3′, probe, FAM 5′ TCAGACCCCAGGCAGTTCCCA 3′ TAMRA; Osteocalcin: f, 5′ CCCTTCCCTGTGCCTGTGTA 3′, r, 5′ CAAAAGCCAAAGCCAATGGA 3′, probe, FAM 5′ CTGTGCCAGAAACCAACCGGCTGA 3′ TAMRA; β-actin was used as control, f, 5′ TGCACCGCAAGTGCTTCTAG 3′, r, 5′ TTTCTGCGCCGTTAGGTTTC 3′, probe, FAM 5′ AGCCAGTGGCGGGACACCCTCT 3′TAMRA. Each specimen was amplified in parallel in five tubes, including gene amplification of PPARγ, CGRP, Runx2, and OC; and internal reference β-actin gene was used as control. A 5-series gradient dilution was used at every amplification time point. A standard curve was drawn, and PCR products were quantified according to the standard curve. The ratios of PPARγ, CGRP, Runx2, and OC to β-actin were viewed as the relative expression of PPARγ, CGRP, Runx2, and OC mRNA, respectively.

Determination of the expression of PPARγ, CGRP, Runx2, and osteocalcin protein by Western blotting

At day 7, the BMSCs were collected and protein was extracted using cell lysis buffer. The bicinchoninic acid (BCA) method was used to determine the total protein content. Samples containing 50 μg protein were separated by 12 % SDS-polyacrylamide gel electrophoresis and β-actin was used as control. The protein was transferred to polyvinylidene difluoride membranes and blocked with 5 % skimmed milk, then incubated with a 1:250 dilution of primary antibodies (mouse anti-rabbit PPARγ polyclonal antibody, mouse anti-rabbit CGRP monoclonal antibody, mouse anti-rabbit Runx2 polyclonal antibody, mouse anti-rabbit OC polyclonal antibody, or mouse anti-rabbit β-actin polyclonal antibody) at 4 °C overnight. After washing with tris-buffered saline containing tween (TBST), the membrane was incubated with a 1:3,000 dilution of goat anti-mouse IgG for 1 h. Membranes were washed again, then ECL reagent was added for 5 min, and the blots were analyzed using a luminescent image analyser (GE healthcare, Piscataway, NJ). The relative expression levels of PPARγ, CGRP, Runx2, and OC protein are presented as the ratio of the gray value of the specific protein to that of β-actin.

Determination of triglyceride (TG) in the cells

At day 14, the content of TG was determined using a triglyceride determination kit (Applygen, China). BMSCs were collected and suspended at a final cell density of 1×10^6 cells/mL in each group. After centrifuging at 1,000 rpm for 10 min, the cells were washed twice with phosphate-buffered saline (PBS) and lysed with 1 % Triton X-100 for 30 min. At the end of the incubation, 3 μL of cytochylema and 300 μL of working solution was added to wells of a 96-well plate, together with blank wells and calibration wells, and incubated at 37 °C for 5 min after

mixing; the absorbance values were measured at a wavelength of 500 nm.

Determination of the content of alkaline phosphatase (ALP), laminin, collagen type I, and osteocalcin in the medium by enzyme-linked immunosorbent assay (ELISA)

At day 14, the content of ALP, laminin, collagen type I, and OC in the medium was determined by ELISA using test kits. BMSCs in each group were collected into 1 mL buffer solution, and centrifuged at 15,000 rpm for 15 min at 4 °C after repeated freeze-thawing treatment to lyse the cells. Standard wells were prepared on the ELISA plates together with standard solution. Next, 40 μL of diluent and 10 μL of supernatant were added to the sample wells, and the plate was incubated at 37 °C for 30 min after mixing, meanwhile blank wells were prepared. After washing 3 times, 50 μL of horseradish peroxidase was added to the sample wells, and the plate was incubated at 37 °C for 30 min. It was then washed another 3 times, 100 μL of chromogenic solution was added, and the plate was incubated at 37 °C for 15 min, at the end of which 50 μL of stop solution was added and the absorbance was measured at a wavelength of 450 nm.

Statistical analysis

All data are expressed as mean ± standard deviation (SD). Data processing was performed by analysis of variance. Pairwise comparisons among groups were performed using multiple comparisons tests. Statistical analysis was performed with SPSS 13.0 software (SPSS Inc., Chicago, IL). A result was considered to be statistically significant at $P < 0.05$.

Results

Identification of BMSCs

Observation of BMSCs under an inverted phase-contrast microscope revealed that they were adherent 24 h after seeding. The adherent BMSCs had adopted a thin spindle-shaped morphology 3 days later when the culture medium was replaced for the first time, and the cells gradually proliferated and became typically spindle-shaped by day 7. By days 12–14, the cells converged and layered, transformed into elliptical or polygonal shapes, and formed whirlpool pattern. The results of cell identification by flow cytometry revealed that BMSCs were positive for CD29, CD44, and CD105 with positive rates of 99.86, 99.34, and 99.65 %, respectively. The cells were negative for CD34 and CD45, with positive rates of 1.27 and 1.45 % (Fig. 1).

Proliferation of BMSCs

The number of cells in each group increased with time in culture. Cell proliferation curves showed the same trend, presenting as an "S" shape, and showing that they entered the exponential phase at day 3. Compared with the normal group, proliferation of the cells in both model and control groups was significantly reduced, and the difference was statistically significant ($P < 0.05$). Proliferation of the cells in both the PPARγ and CGRP groups was also lower than the normal group, but no significant difference was observed ($P > 0.05$). Cell proliferation in the double group was slightly lower than that in the normal group, but there was no significant difference between them ($P > 0.05$). The proliferation of the cells in all groups tended to slow down at day 6 and cell proliferation entered a plateau period (Fig. 2).

Expression of PPARγ, CGRP, Runx2, and osteocalcin mRNA

At day 7, the expression level of PPARγ mRNA in the model, control, and CGRP groups was significantly higher than that in the normal group ($P < 0.05$); the expression of PPARγ mRNA in the PPARγ and double groups was similar to that in the normal group, with no significant differences observed ($P > 0.05$). CGRP mRNA was expressed at similar levels in the CGRP and double groups ($P > 0.05$), and no CGRP mRNA was detected in any of the other groups. The expression level of Runx2 and OC mRNA in the model and control groups was significantly lower than that in the normal group ($P < 0.05$), while expression of both mRNAs in the PPARγ and CGRP groups was similar to the normal group ($P > 0.05$). Expression of Runx2 and OC in the double group was higher than in the normal group, and the difference was statistically significant ($P < 0.05$) (Fig. 3).

Expression of PPARγ, CGRP, Runx2, and osteocalcin protein

At day 7, immunoblotting showed that the bands of PPARγ protein in the model, control, and CGRP groups were significant denser than that in the normal group ($P < 0.05$); the density of the PPARγ protein bands in the PPARγ and double groups was similar to that in the normal group, and there were no significant differences among the PPARγ, double, and normal groups ($P > 0.05$). CGRP protein was expressed in both the CGRP and double groups, and the band intensity was similar between them, with no

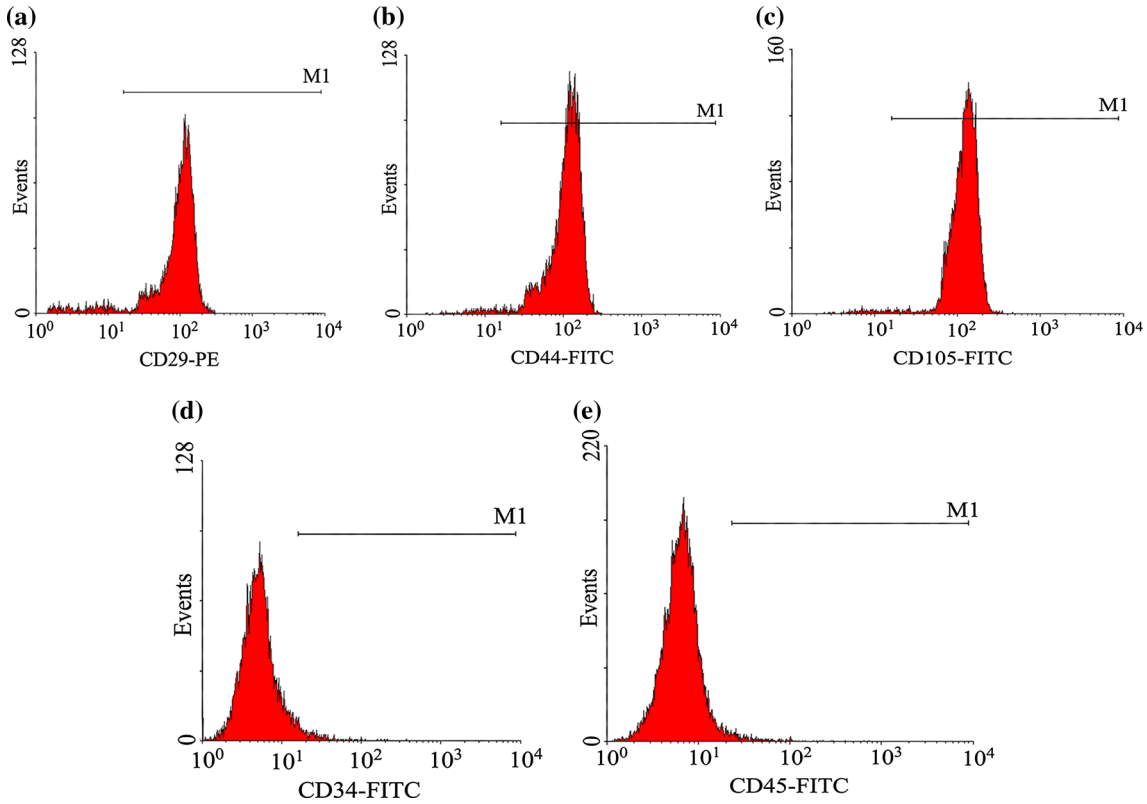

Fig. 1 The flow cytometry result of BMSCs. BMSCs were analyzed by flow cytometry at the third passage using antibodies CD29 (**a**), CD44 (**b**), CD105 (**c**), CD34 (**d**), and CD45 (**e**). BMSCs were positive for CD29, CD44, and CD105; and negative for CD34 and CD45

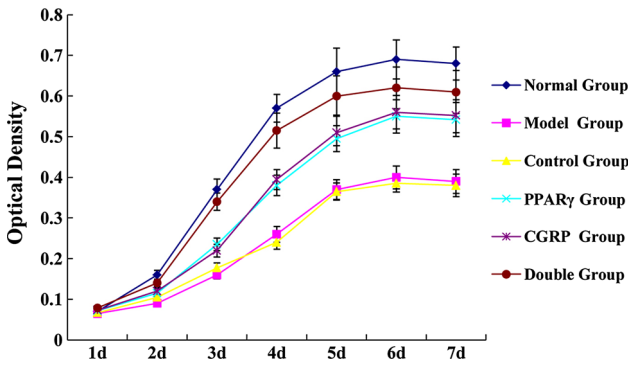

Fig. 2 Result of the MTT proliferation assay. *Normal Group* BMSCs without treatments. *Model Group* BMSCs induced with alcohol only. *Control Group* BMSCs transfected with empty pGFP-V-RS vector, and induced with alcohol. *PPARγ Group* BMSCs transfected with silencing vector pGFP-V-RS-siPPARγ, and induced with alcohol. *CGRP Group* BMSCs transfected with the expression vector pGFP-V-RS-exCGRP, and induced with alcohol. *Double Group* BMSCs transfected with the double-gene vector pGFP-V-RS-siPPARγ-ex-CGRP, and induced with alcohol. The proliferation curve of the cells in all groups showed similar "*S*" shape trend. Compared with the normal group, proliferation potential of cells in the model group and control group was significantly reduced ($P < 0.05$). Proliferation potential of the cells in the PPARγ and CGRP groups was also lower than that in normal group, but with no significant difference ($P > 0.05$). Cell proliferation in double group was also lower than that in the normal group, but with no significant difference ($P > 0.05$)

significant differences observed ($P > 0.05$); no CGRP protein was detected in other groups. The levels of Runx2 and OC protein in the model and control groups were significantly lower than that in the normal group ($P < 0.05$), while in the PPARγ and CGRP groups levels were similar to that in the normal group, with no significant differences observed. In contrast, the bands of Runx2 and OC protein in the double group were significantly denser than in the normal group ($P < 0.05$) (Fig. 4).

Cell content of TG

At day 14, the content of TG in each of the model, control, and CGRP groups was significantly higher than in the normal group ($P < 0.05$). The TG content of the PPARγ and double groups was similar to the normal group, and there was no significant difference among the PPARγ, double, and normal groups ($P > 0.05$) (Fig. 5).

Cell activity of ALP

At day 14, the activity of ALP in the model and control groups was significantly lower than that in the normal group, ($P < 0.05$). ALP activity in the PPARγ and CGRP groups was similar to that in the normal group, with no

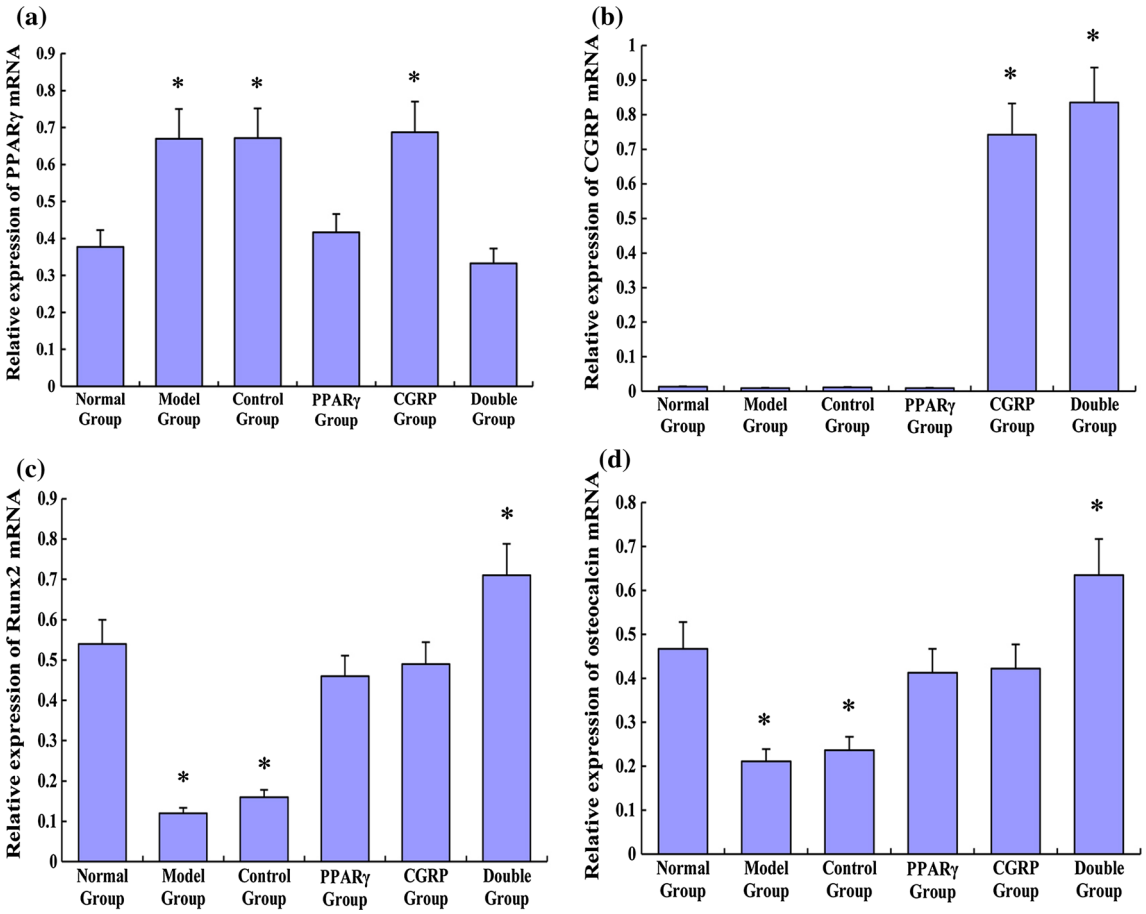

Fig. 3 Expression levels of PPARγ, CGRP, Runx2, and osteocalcin mRNA at day 7. **a** Expression of PPARγ mRNA in the model, control, and CGRP groups was significantly higher than that in the normal group ($*P < 0.05$); expression of PPARγ mRNA in both the PPARγ and double groups was similar to that in the normal group. There is no significant difference ($P > 0.05$). **b** Expression of CGRP mRNA in the CGRP and double groups at a similar level. No significant difference was found ($P > 0.05$). No CGRP mRNA was detected in other groups. **c**, **d** Expression of Runx2 and osteocalcin mRNA in the model and control groups was significantly lower than that in the normal group ($*P < 0.05$). In the PPARγ and CGRP groups, it was similar to that in the normal group and no significant difference was found ($P > 0.05$). Expression of Runx2 and osteocalcin mRNA in the double group was significantly higher than that in the normal group ($*P < 0.05$)

statistically significant difference between them ($P > 0.05$). ALP activity in the double group was significantly higher than that in the normal group ($P < 0.05$) (Fig. 6).

Osteocalcin content in the medium

At day 14, the OC content of the medium in the model and control groups was significantly lower than that in the normal group ($P < 0.05$). The OC content of the medium in the PPARγ and CGRP groups was similar to that in the normal group, and the difference was not statistically significant ($P > 0.05$). In contrast, the OC content in the medium in the double group was significantly higher than that in the normal group ($P < 0.05$) (Fig. 7).

Laminin content of the cells

At day 14, the laminin content of the model and control groups was significantly lower than that in the normal group ($P < 0.05$), while that of the PPARγ and CGRP groups was similar to that in the normal group, and the difference was not statistically significant ($P > 0.05$). The laminin content of the double group was significantly higher than that in the normal group ($P < 0.05$) (Fig. 8).

Collagen type I content of the cells

At day 14, the collagen type I content of cells in the model and control groups was significantly lower than that in the normal group ($P < 0.05$). While the collagen type I content in the PPARγ and CGRP groups was similar to that in the

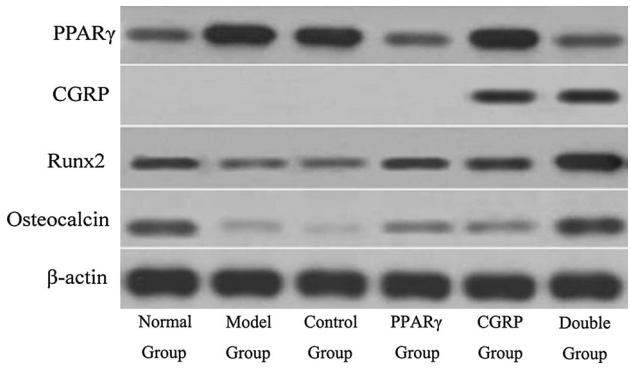

Fig. 4 Expression levels of PPARγ, CGRP, Runx2, and osteocalcin protein at day 7. The bands of PPARγ protein in the model, control, and CGRP groups were significantly denser than that in the normal group ($P < 0.05$); the density of PPARγ protein in the PPARγ and double groups were similar to that in the normal group ($P > 0.05$). CGRP protein was expressed in both CGRP and double groups, and the band intensity was similar. No significant difference is found between these two groups ($P > 0.05$); No CGRP protein expression was detected in other groups. The density of Runx2 and osteocalcin protein bands in model and control groups was significantly lower than that in the normal group ($P < 0.05$); while the PPARγ and CGRP group were similar to the normal group ($P > 0.05$). The bands of Runx2 and osteocalcin protein in the double group were significantly denser than that in the normal group ($P < 0.05$)

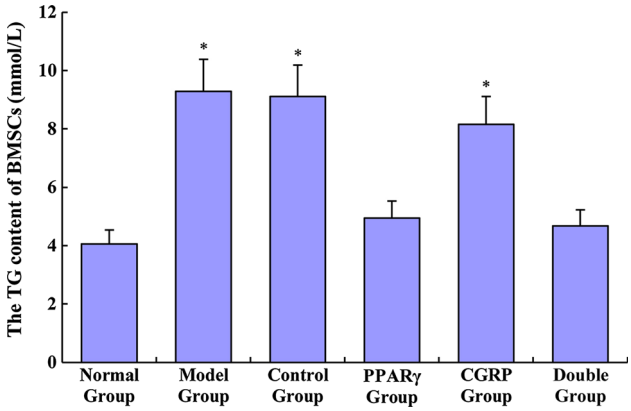

Fig. 5 Triglyceride content of the cells at day 14. The TG content of the model, control, and CGRP groups was significantly higher than that in the normal group (*$P < 0.05$). In the PPARγ and double groups, it was similar to the normal group and there was no significant difference ($P > 0.05$)

normal group, with no statistically significant difference ($P > 0.05$). In the double group, it was significantly higher than that in the normal group ($P < 0.05$) (Fig. 9).

Discussion

As a bioactive peptide, CGRP consists of 37 amino acid residues, and is mainly synthesized in small sensory neurons in the dorsal root ganglion [18]. CGRP-positive nerve

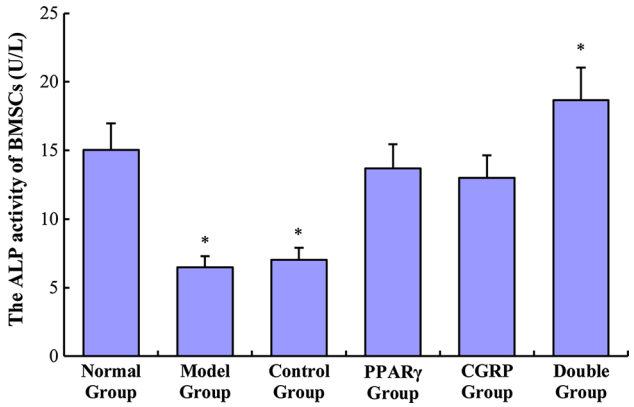

Fig. 6 ALP activity of cells at day 14. The ALP activity in the model and control groups was significantly lower than that in the normal group (*$P < 0.05$). ALP activity in the PPARγ and CGRP group was similar to that in the normal group and there was no significant difference ($P > 0.05$). ALP activity in the double group is significantly higher than that in the normal group (*$P < 0.05$)

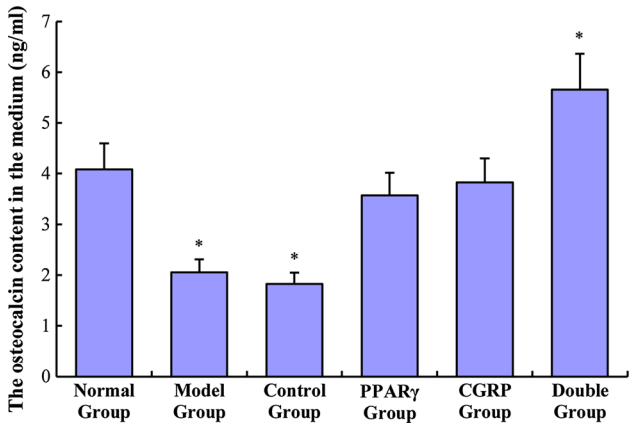

Fig. 7 Osteocalcin content in the medium at day 14. The osteocalcin content in the medium in the model and control groups was significantly lower than that in the normal group (*$P < 0.05$). The osteocalcin content in the medium in the PPARγ and CGRP groups was similar to that in the normal group. There was no significant difference ($P > 0.05$). Osteocalcin content in the medium in the double group was significantly higher than that in the normal group (*$P < 0.05$)

fibers are abundantly distributed in bone tissue, and closely related to the growth and development of bone [19, 20]. In neonatal rat, the number of CGRP-positive nerve fibers significantly increases around the femoral metaphysis. They decrease around the femoral metaphysis with time, but gradually increase again around the epiphysis [21]. By four weeks after birth, CGRP-positive nerve fibers around the femoral epiphysis are more abundant than that around the femoral metaphysis, and extend along toward the epiphyseal trabeculae. These findings indicate that CGRP is involved in the growth and development of bone. In the process of fracture healing, CGRP-positive nerve fibers regularly increase in the periosteum as well as in new bone

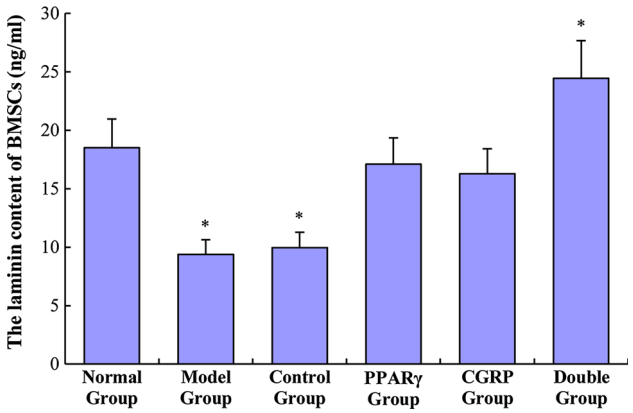

Fig. 8 Laminin content of the cells at day 14. The laminin content of cells in the model and control groups was significantly lower than that in the normal group ($*P < 0.05$). In the PPARγ and CGRP groups, it was similar to that in the normal group and there was no significant difference ($P > 0.05$). In the double group, it was significantly higher than that in the normal group ($*P < 0.05$)

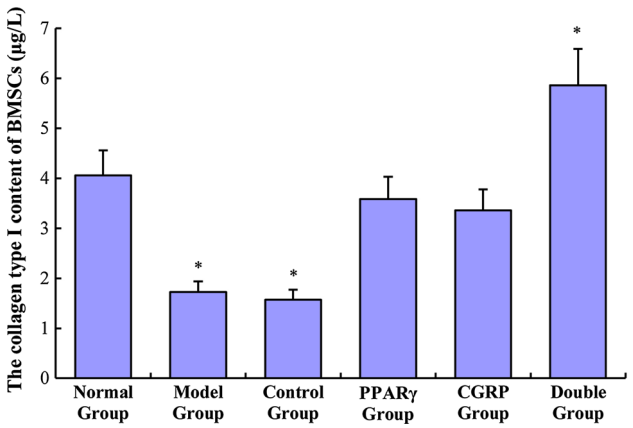

Fig. 9 The collagen type I concentration of cells at day 14. The collagen type I content of the model and control groups was significantly lower than that in the normal group ($*P < 0.05$). In contrast, the collagen type I content in the PPARγ and CGRP groups was similar to that in the normal group and there was no significant difference ($P > 0.05$). When compared to that in the normal group, the double group was significantly higher ($*P < 0.05$)

tissue and granulation tissue, which indicates that CGRP-positive nerve fibers are closely related to the process of bone repair [22, 23].

PPARγ is a specific transcription factor closely involved in the induction of adipogenic differentiation, which has an important regulatory effect on adipocyte differentiation in adipose tissue. It appears prior to activation of many other adipocyte genes during adipogenic differentiation and induces stem cells to differentiate into adipocytes, which could affect the storage of fatty acids in adipose tissue. Previous studies have demonstrated that alcohol can stimulate increased expression of PPARγ mRNA in BMSCs. Upregulation of PPARγ can promote adipogenic differentiation and inhibit the osteogenic differentiation of BMSCs, which consequently leads to increased lipid generation and decreased bone formation. The accumulation of fatty tissue can compromise blood circulation in the femoral head and eventually result in ONFH. Downregulation of PPARγ expression may inhibit the adipogenic differentiation of BMSCs, and thus maintain the osteogenic differentiation potential of the cells, which may potentially reduce the incidence of alcohol-induced ONFH [24–26].

Numerous studies have shown that OC synthesized in BMSCs is mostly secreted into the culture medium. Cells' OC expression is parallel with their osteogenic differentiation, which can be thought as a characteristic marker of osteogenic differentiation. The increase in ALP activity is also an early marker for osteogenic differentiation of BMSCs. Both of these markers are routinely used as an important indication for in vitro osteogenic differentiation [27]. Runx2, referred as core-binding factor al (Cbfal), is considered to be the key transcription factor which is involved in osteoblast differentiation [28, 29]. It plays double roles in adipogenic differentiation and osteogenic differentiation of BMSCs. Therefore, Runx2 has a positive regulatory effect on bone formation. PPARγ inhibits the expression of Runx2 while promoting adipogenic differentiation of BMSCs, which leads to decreased osteogenesis [30]. Phillips and colleagues showed that the occurrence of steroid-induced ONFH is mainly caused by inhibition of Runx2 activity [31]. Han also showed that CGRP can promote the expression of Runx2 [32]. Laminin is a type of soluble macromolecular glycoprotein which regulates the cell adhesion mediated by proteoglycan and integrin, which regulate cell growth and differentiation. Collagen type I is a specific type of collagen synthesized by osteoblasts in bone tissue. Laminin and collagen type I together play an important role in osteoblastic differentiation of BMSCs [33, 34].

In this study, we observed that combined regulation of PPARγ and CGRP genes inhibited alcohol-induced adipogenic differentiation of BMSCs. In the PPARγ group, BMSCs were transfected with the silencing vector pGFP-V-RS-siPPARγ. The cells' proliferation was slightly decreased than that in the normal group and there is no significant difference when two groups were compared ($P > 0.05$). There was no significant difference when comparing PPARγ group to normal group regarding to the expression of PPARγ, Runx2, and OC in both mRNA and protein levels ($P > 0.05$). There was no significant difference in TG content, ALP activity, content of laminin, collagen type I, and OC in the medium when compared to that in the normal group ($P > 0.05$). These results indicate that siRNA targeting PPARγ is able to suppress the expression of PPARγ mRNA and protein, and inhibit alcohol-induced adipogenic differentiation; while maintaining the osteogenic differentiation characteristics of BMSCs.

In the CGRP group, BMSCs were transfected with the expression vector pGFP-V-RS-exCGRP. Cells' proliferation was slightly lower than that in the normal group and there is no significantly difference ($P > 0.05$). Expression of PPARγ mRNA, protein, and TG content were all significantly higher than that in the normal group ($P < 0.05$); while Runx2, OC mRNA and protein, ALP activity, the content of laminin, collagen type I, and OC in the medium were similar to that in the normal group ($P > 0.05$). These results indicate that the expression of CGRP promotes osteogenic differentiation and partially reverses the effect of alcohol-induced adipogenic differentiation of BMSCs, without significantly reducing the potential of cell proliferation and osteogenic differentiation.

In the double group, BMSCs were transfected with the double-gene vector pGFP-V-RS-siPPARγ-exCGRP. Cells' proliferation was almost the same as that in the normal group ($P > 0.05$), and CGRP mRNA and protein were stably expressed. Expression of PPARγ mRNA, protein, and TG content were similar to the normal group, there is no significant difference ($P > 0.05$). The levels of Runx2, OC mRNA and protein; ALP activity; the content of laminin, collagen type I, and OC in the medium were all significantly higher than that in the normal group ($P < 0.05$). These results indicate that combined regulation of PPARγ and CGRP genes can efficiently block PPARγ gene expression of BMSCs, which suppressed adipogenic differentiation and improved osteogenic potential of the cells.

Taken together, these results provide evidence as a novel approach for the prevention of ONFH.

Acknowledgments This study was supported by the National Natural Science Foundation of China (No. 81171776).

Conflict of interest The authors have declared that no competing interest exists.

References

1. Wang YS, Li YB, Mao KY, Li J, Cui QJ, Wang GJ (2003) Alcohol-induced adipogenesis in bone and marrow: a possible mechanism for osteonecrosis. Clin Orthop Relat Res 410:213–224
2. Kim MH, Cho GW, Huh YM, Kim SH (2010) Transduction of human EPO into human bone marrow mesenchymal stromal cells synergistically enhances cell-protective and migratory effects. Mol Biol (Mosk) 44:656–663
3. Zhang L, Zheng W, Wang Y, Wang Y, Huang H (2013) Human bone marrow mesenchymal stem cells support the derivation and propagation of human induced pluripotent stem cells in culture. Cell Reprogr 15:216–223
4. Agata H, Asahina I, Watanabe N, Ishii Y, Kubo N, Ohshima S, Yamazaki M, Tojo A, Kagami H (2010) Characteristic change and loss of in vivo osteogenic abilities of human bone marrow stromal cells during passage. Tissue Eng Part A 16:663–673
5. Edamura K, Kuriyama K, Kato K, Nakano R, Teshima K, Asano K, Sato T, Tanaka S (2012) Proliferation capacity, neuronal differentiation potency and microstructures after the differentiation of canine bone marrow stromal cells into neurons. J Vet Med Sci 74:923–927
6. Post S, Abdallah BM, Bentzon JF, Kassem M (2008) Demonstration of the presence of independent pre-osteoblastic and pre-adipocytic cell populations in bone marrow-derived mesenchymal stem cells. Bone 43:32–39
7. Curtis KM, Gomez LA, Schiller PC (2012) Rac1b regulates NT3-stimulated Mek-Erk signaling, directing marrow-isolated adult multilineage inducible (MIAMI) cells toward an early neuronal phenotype. Mol Cell Neurosci 49:138–148
8. Steger DJ, Grant GR, Schupp M, Tomaru T, Lefterova MI, Schug J, Manduchi E, Stoeckert CJ Jr, Lazar MA (2010) Propagation of adipogenic signals through an epigenomic transition state. Genes Dev 24:1035–1044
9. Arck P, Toth B, Pestka A, Jeschke U (2010) Nuclear receptors of the peroxisome proliferator-activated receptor (PPAR) family in gestational diabetes: from animal models to clinical trials. Biol Reprod 83:168–176
10. Hong JH, Hwang ES, McManus MT, Amsterdam A, Tian Y, Kalmukova R, Mueller E, Benjamin T, Spiegelman BM, Sharp PA, Hopkins N, Yaffe MB (2005) TAZ, a transcriptional modulator of mesenchymal stem cell differentiation. Science 309:1074–1078
11. Park KW, Waki H, Choi SP, Park KM, Tontonoz P (2010) The small molecule phenamil is a modulator of adipocyte differentiation and PPARgamma expression. J Lipid Res 51:2775–2784
12. Takada I, Kouzmenko AP, Kato S (2009) Wnt and PPARgamma signaling in osteoblastogenesis and adipogenesis. Nat Rev Rheumatol 5:442–447
13. Li X, Cui Q, Kao C, Wang GJ, Balian G (2003) Lovastatin inhibits adipogenic and stimulates osteogenic differentiation by suppressing PPARgamma2 and increasing Cbfa1/Runx2 expression in bone marrow mesenchymal cell cultures. Bone 33:652–659
14. Tsujikawa K, Yayama K, Hayashi T et al (2007) Hypertension and dysregulated proinflammatory cytokine production in receptor activity-modifying protein 1-deficient mice. Proc Nati Acad Sci USA 104:16702–16707
15. Lerner UH (2006) Deletions of genes encoding calcitonin/alpha-CGRP, amylin and calcitonin receptor have given new and unexpected insights into the function of calcitonin receptors and calcitonin receptor-like receptors in bone. J Musculoskelet Neuronal Interact 6:87–95
16. Wang YS, Wang YH, Zhao GQ, Li YB (2011) Osteogenic potential of human calcitonin gene-related peptide alpha gene-modified bone marrow mesenchymal stem cells. Chin Med J 124:3976–3981
17. Deng W, Bivalacqua TJ, Chattergoon NN, Jeter JR Jr, Kadowitz PJ (2004) Engineering ex vivo-expanded marrow stromal cells to secrete calcitonin gene-related peptide using adenoviral vector. Stem Cells 22:1279–1291
18. Li J, Kreicbergs A, Bergström J, Stark A, Ahmed M (2007) Site-specific CGRP innervation coincides with bone formation during fracture healing and modeling: a study in rat angulated tibia. J Orthop Res 25:1204–1212
19. Tsujikawa K, Yayama K, Hayashi T, Matsushita H et al (2007) Hypertension and dysregulated proinflammatory cytokine production in receptor activity-modifying protein 1-deficient mice. Proc Nati Acad Sci USA 104:16702–16707
20. Imai S, Matsusue Y (2002) Neuronal regulation of bone metabolism and anabolism: calcitonin gene-related peptide-, substance P-, and tyrosine hydroxylase-containing nerves and the bone. Microsc Res Tech 58:61–69

21. Hara-Irie F, Amizuka N, Ozawa H (1996) Immunohistochemical and ultrastructural localization of CGRP-positive nerve fibers at the epiphyseal trabecules facing the growth plate of rat femurs. Bone 18:29–39
22. Hukkanen M, Konttinen YT, Santavirta S, Paavolainen P, Gu XH, Terenghi G, Polak JM (1993) Rapid proliferation of calcitonin gene-related peptide-immunoreactive nerves during healing of rat tibial fracture suggests neural involvement in bone growth and remodelling. Neuroscience 54:969–979
23. Aoki M, Tamai K, Saotome K (1994) Substance p-related and calcitonin-gene-related peptide- immunofluorescent nerves in the repair of experimental bone defects. Int Orthop 18:317–324
24. Cui QJ, Wang YS, Saleh KJ, Wang GJ, Balian G (2006) Alcohol-induced adipogenesis in a cloned bone-marrow stem cell. J Bone Joint Surg Am 88:148–154
25. Liu M, Wang YS, Li YB, Zhao GQ (2012) Construction and identification of the recombinant adenovirus vector carrying a small interfering RNA targeting the peroxisome proliferator-activated receptor-γ. Chin Med J (Engl) 125:671–675
26. Yin L, Li YB, Wang YS (2006) Dexamethasone-induced adipogenesis in primary marrow stromal cell cultures: mechanism of steroid-induced osteonecrosis. Chin Med J (Engl) 119:581–588
27. Wang YS, Yin L, Li YB, Liu PL, Cui QJ (2008) Preventive effects of puerarin on alcohol-induced osteonecrosis. Clin Orthop 466:1059–1067
28. Dong SW, Ying DJ, Duan XJ, Xie Z, Yu ZJ, Zhu CH, Yang B, Sun JS (2009) Bone regeneration using an acellular extracellular matrix and bone marrow mesenchymal stem cells expressing Cbfa1. Biosci Biotechnol Biochem 73:2226–2233
29. Tu Q, Zhang J, James L, Dickson J, Tang J, Yang P, Chen J (2007) Cbfa1/Runx2-deficiency delays bone wound healing and locally delivered Cbfa1/Runx2 promotes bone repair in animal models. Wound Repair Regen 5:404–412
30. Jeon MJ, Kim JA, Kwon SH, Kim SW, Park KS, Park SW, Kim SY, Shin CS (2003) Activation of peroxisome proliferator-activated receptor-gamma inhibits the Runx2-mediated transcription of osteocalcin in osteoblasts. J Biol Chem 278:23270–23277
31. Phillips JE, Gersbach CA, Wojtowicz AM, García AJ (2006) Glucocorticoid-induced osteogenesis is negatively regulated by Runx2/Cbfal serine phosphorylation. J Cell Sci 119:581–591
32. Han N, Jiang BG, Wang TB, Zhang PX, Kou YH, Zhang DY (2011) Effect of calcitonin gene-related peptide on RUNX2 expression in primary rat osteoblasts. Beijing Da Xue Xue Bao (Chin) 43:652–656
33. Mittag F, Falkenberg EM, Janczyk A, Götze M, Felka T, Aicher WK, Kluba T (2012) Laminin-5 and type I collagen promote adhesion and osteogenic differentiation of animal serum-free expanded human mesenchymal stromal cells. Orthop Rev (Pavia) 4:e36
34. Salasznyk RM, Klees RF, Boskey A, Plopper GE (2007) Activation of FAK is necessary for the osteogenic differentiation of human mesenchymal stem cells on laminin-5. J Cell Biochem 100:499–514